Polarimetric Weather Radar Calibration by Computational Electromagnetics

Djordje Mirkovic
Cooperative Institute for Mesoscale Studies
National Severe Storms Laboratory (NOAA)
Norman, OK
Djordje.Mirkovic@noaa.gov

Dusan S. Zrnic
National Severe Storms Laboratory (NOAA)
Norman, OK
Dusan.Zrnic@noaa.gov

***Abstract*—The paper proposes a technique for calibrating a large polarimetric phased array weather radar The focus is on the use of computational electromagnetics. It validates the accuracy of the computations on a scaled-down antenna model and derives calibration parameters for the same model. The proposed technique is demonstrated using the WIPL-D software. The calibration is illustrated with all mathematical concepts required to carry the calibration out. The concept is adapted to use the results of numerical simulations which is part of the paper's novelty. Additionally, a roadmap of polarimetric phased array calibration is proposed and illustrated.**

Keywords—calibration, polarimetric weather radar, polarimetric weather radar calibration, radar.

I. INTRODUCTION

The current national weather radar surveillance network uses dual-polarized dish antennas. The aging network's lifetime is being extended for another twenty years through replacement of obsolete parts and inclusion of modern technology. Thus, it is expected that in about ten years a path for possible replacement should be firmed up to fall in line with typical manufacturing/procurement timeline. The new generation radar should provide the same quality weather data while serving the multifunction capability and efficiently using the allocated frequency spectrum.

Quality of the polarimetric data available from the WSR-88D radar is a benchmark for any new generation radar. Requirements on the polarimetric variables include differential reflectivity bias less than 0.1 dB, copolar correlation coefficient bias of less than 0.01 and cross-polar isolation in the antenna of more than 40 dB for the current operation mode (simultaneous horizontal H and vertical V polarization on transmission and reception). These requirements are satisfied by the WSR-88D's dish antenna whose cross-polar radiation patterns experience null collocated with the co-polar peak, while the cross-polar peaks exhibit four symmetric lobes with respect to the main beam axis. The phases of adjacent lobes are offset from each other by 180 degrees. These antenna properties are invariant with respect to the pointing directions.

Initiatives for development of new generation weather radar are multi-agency efforts aimed toward the Multifunction Phased Array Radar (MPAR) and Spectrum Efficient National Surveillance Radar (SENSR).

Both initiatives consider multiple system architectures. One radar candidate is the Planar Phased Array Radar (PPAR), a program developed jointly by the National Oceanic and Atmospheric Administration (NOAA), Lincoln Laboratory (LL), and the Federal Aviation Administration (FAA). The PPAR is chosen as one of the most mature phased array technologies due to its wide use in the military. Previously, the technology transfer has already happened with single polarization phased array radar at the National Weather Radar Testbed (NWRT) [1]. Studies on this radar proved that electronic scanning strategies of the PPAR can achieve faster, adaptive scanning and avoid mechanical wear typical for radars with dish antennas. However, this capability of the PPAR comes at the price which specifically affects the dual-pol estimates and makes the calibration of the PPAR orders of magnitude more complex than that of the dish antenna radars.

The paper is organized as follows. In the second section is the overview of existing calibration techniques and the mathematical formulation of the calibration parameters. The third section evaluates the accuracy of the computational electromagnetic (CEM) modeling for the application in PPAR calibration. The fourth section describes how to adapt CEM results to the calibration problem and finally, the fifth section presents biased radar measurements and model simulated bias.

II. CALIBRATION PROBLEM

The calibration of the PPAR has to address multiple issues related to the dependence of antenna patterns and orientation of electric fields within the beam. The main calibration issues are orthogonality and orientation of the electric fields produced by the antenna; geometrically induced cross-polar fields (geometrical coupling) [2], cross-polar (unwanted) radiation and match of the H and V beam cross-sections and pointing direction [3].

Gathering necessary calibration information may be achieved by various techniques [4]. These are based either on Far-field (FF) and Near-field (NF) measurements or simulations [4]. To our knowledge, these techniques are limited and/or not fully developed. They typically include an initial full NF antenna measurement and calibration with the placement of a near-field probe in the vicinity of the radar antenna for the antenna/probe cross-coupling measurement. Calibration is done using the initial NF measurement and cross-coupling measurement between the probe and antenna, assuming the initial NF radiation patterns. The proposed FF techniques

Submitted On: September 28, 2018
Accepted On: October 3, 2018

1054-4887 © ACES

$$\begin{vmatrix} V_1 \\ V_2 \end{vmatrix} = C \begin{vmatrix} (s_h \cos^2\gamma + s_v \sin^2\gamma) g_1 W_1 + (s_h \cos\gamma \sin\psi + s_v \sin\gamma \cos\psi)\sqrt{g_1}\sqrt{g_2} C_T e^{j\beta} W_1 \\ (s_h \cos\gamma \sin\psi + s_v \sin\gamma \cos\psi)\sqrt{g_1}\sqrt{g_2} C_T e^{j\xi} W_1 + (s_h \sin^2\gamma + s_v \cos^2\psi) g_2 C_T C_R e^{j(\beta+\xi)} W_1 \end{vmatrix}. \quad (1)$$

require towers or drones to measure radiation patterns often enough to catch the effects of failing radiating elements [4]. These patterns are used to create the calibration matrix.

Simulation-based techniques, on the other hand, have the ability to address and evaluate issues inherent to the PPAR technology that otherwise cannot be evaluated (i.e., departure from intended polarization while beam-steering). The capability of the numerical models to precisely replicate PPAR antenna field characteristics is illustrated in the next section.

The calibration problem can be set by the voltage on reception for polarimetric PPAR (1) [3]. The Eq. 1 assumes the cross-polar radiation pattern coaxial to the copolar pattern. The cross-polar pattern may be due to cross polar sides of the patch radiator or due to the squinting of the electric field vector caused by geometry (i.e., pointing direction is out of the principal plane) [3], [5]. The effective squinting angles ψ, γ determine the orthogonal components of the electric field. This formulation yields nine calibration parameters [3], namely: antenna gains g_1, g_2; electric field squinting angles (i.e., angles of intended "horizontal" and "vertical" components with respect to the horizontal and quasi-vertical direction) ψ, γ ; radar system parameter C and calibration for port one and port two paths for same input on transmit $C_T e^{j\beta} = \frac{W_2}{W_1}$ (i.e., the ratio of transmitted voltages at ports 1 and 2); and receive $C_R e^{j\xi} = \frac{V_2}{V_1}$ (ratio of received voltages at port 1 and port 2). The thransmission differential phase β consists of the part in the transmitter and part in the antenna. Similarly ξ has two components, one from the antenna the other from the receiver. Here, we consider the antenna differential phases and differential reflectivities.

The differential reflectivity is useful for classifying precipitation type and gauging amounts [6]. Therefore it should be free of biases by the radar system. The differential phase is important for measurements of rain [7] and for identification of large hail [8]. Quantitative precipitation measurements use range derivatives of differential phase hence are not affected by the system induced bias. Nonetheless, proper unwrapping of differential phase hinges on the knowledge of the system phase. Also, the system differential phase is required to determine the differential phase on backscattering by large scatterers such as hail or biota.

In the remainder of the paper, we focus on the antenna parameters contributing to the bias in the polarimetric variables. Furthermore, we consider only calibration in the principal planes, where the cross-polar radiation is negligible, and geometrical bias is null. Nonetheless, our approach is applicable for any pointing direction for which radiation patterns are available.

III. Antenna Modeling and Validation

Achieving the strict calibration requirements set by the current WSR-88D radar is challenging for any proposed technique. In order to achieve it, the measurement, as well as the simulation results, must replicate the true antenna patterns very accurately. Here we use a single panel of the proposed PPAR demonstrator (Ten Panel Demonstrator – TPD) radar to evaluate the accuracy of the antenna modeling.

The radiating element of the TPD is a 3 layer stacked patch antenna. The precise antenna model was developed and simulated in the WIPL-D Pro software. The single antenna

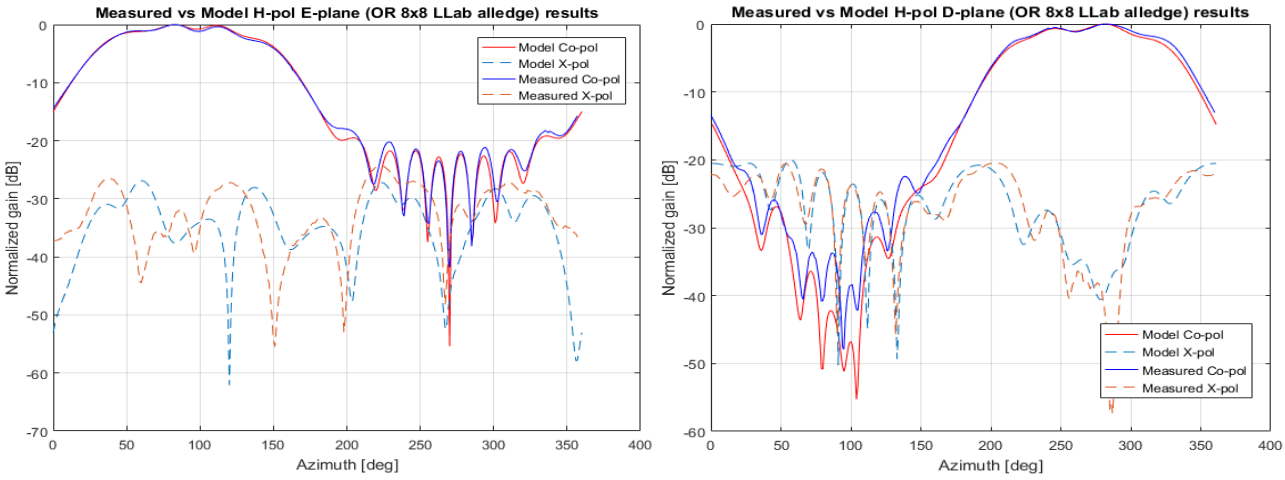

Fig. 1. Modeled and measured radiation patterns. The H-polarized element in the lover left quadrant of a single 8x8 panel is excited and the other elements terminated. Left: in the E-plane and Right: in the D-plane.

panel consists of 64 radiating elements. The panel under test uses one of four central elements for each of the polarizations (H, V, RHCP, LHCP), while others are terminated. Measurements were made at the Advanced Radar Research Center (ARRC) anechoic chamber using the Agilent network analyzer (N5222A).

The measurements include copolar and cross-polar radiation patterns as shown in Fig. 1. The patterns were obtained in the E field plane, H field plane and Diagonal plane, but for brevity, only patterns in the E and D plane are presented in Fig. 1. Very good agreement between the copolar patterns for both cuts is observed, while the cross-polar component in the E-plane shows a slight discrepancy compared to the model. In the D-plane the cross-polar components agree well. The discrepancy between the cross-polar results in the E-plane is most likely caused by the spurious reflections in the chamber.

IV. Computational Electromagnetics (CEM) as an Approach to Calibration

The CEM may be used for obtaining radiation properties of the large PPAR antenna. Yet the CEM softwares are limited by the maximal antenna size they can handle. Software packages that are currently available can exactly solve arrays which consist of a few hundred radiators, whereas the larger arrays are typically solved using some of the approximative techniques. It is not known if the accuracy of these approximative techniques is sufficient to provide polarimetric variables with acceptable errors. Some attempts have been made to evaluate the accuracy, yet a full systematic study is still pending [4]

Herein a TPD radar with an antenna consisting of 640 radiating elements is considered for CEM based calibration. This antenna size is an upper limit which may be solved in a reasonable amount of time without application of approximation techniques. The goal is to simulate patterns and develop calibration parameters that may be used to correct biased radar observations and isolate sources and causes of these biases. Evaluation of the calibration parameters follows directly from the simulation output results. Under the assumption that the antenna is oriented according to Ludwig 2 definition for radiation, or more precisely, E_φ and E_θ components of the radiated field are copolar and cross-polar components of the intended radiation. Depending on the intended polarization, the calculated fields determine the copolar or cross-polar radiation pattern of the antenna. For this case calibration parameters can be calculated as:

$$\arctan\psi = \frac{f_{hv}}{f_{vv}};\ \arctan\gamma = \frac{f_{vh}}{f_{hh}};\ Gdiff = \frac{g_1}{g_2} = \frac{|f_{hh}|^2}{|f_{vv}|^2}$$
$$\beta = \frac{\arg(f_{vv}^{Tx})}{\arg(f_{hh}^{Tx})} + K_{backend}\ ;\ \xi = \frac{\arg(f_{vv}^{Rx})}{\arg(f_{hh}^{Rx})} + K_{backend}\ . \quad (2)$$

Where $f_{hh}, f_{vh}, f_{hv}, f_{vv}$ are values of the voltage radiation patterns at the beam-center. The remaining C, C_T, C_R and the $K_{backend}$ parameters depend only on the back-end of the antenna and cannot be addressed by the antenna simulation. These parameters are expected to be invariant to the pointing direction of the array. Important to notice is that geometrical bias and cross-polarization bias are not included in the formulation of the problem. Nevertheless, for simulations using

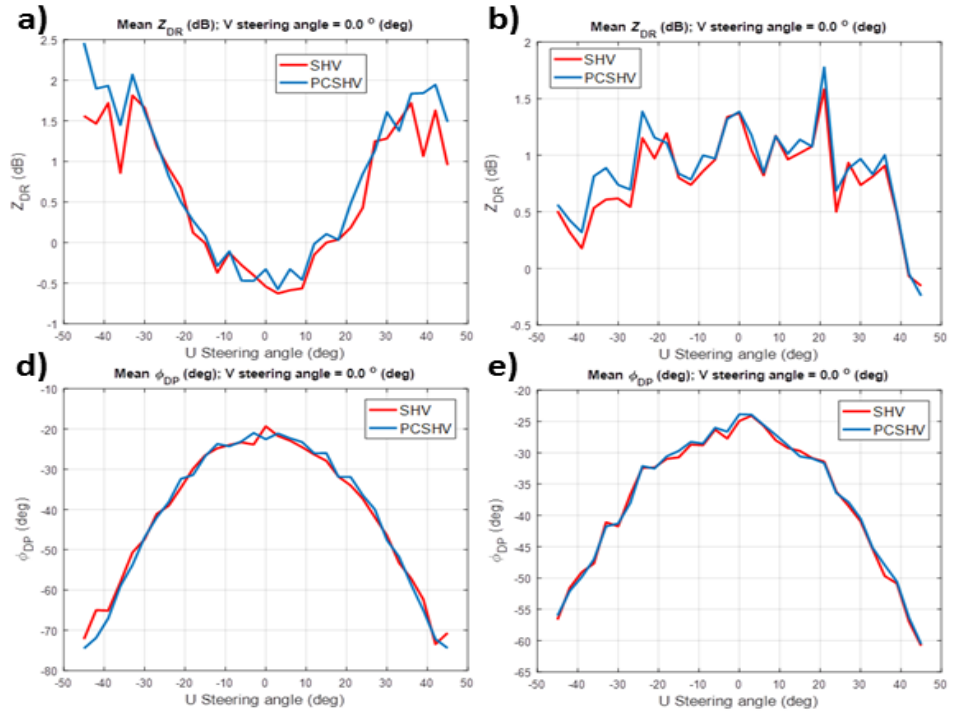

Fig. 2. Measured differential reflectivity (top) and differential phase (bottom) in light rain showing bias in the polarimetric variables when broadside is pointed at zenith angle (left) and when the principal plane is slightly off vertical (right). At zenith angle 3mm of water accumulated at the top of the radome. Water was not present (except for droplets) in the latter case. SHV denotes simultaneus transmission and reception of H and V polarization; PCSHV stands for pulse coded SHV. Coding reduces signal cross-copling and ensures minimal system bias. Figure coutery (I. Ivic).

the Ludwig 2 definition all bias sources (mechanisms) are incorporated in the E_φ and E_θ field components.

V. Radar Bias Measurements and Simulation

Observations that served as motivation for the study were collected using the TPD radar in light rain during spring 2016. The radar was operated with the beam scanning in the principal plane. In one case, the broadside was pointing at the zenith (zenith mode) and in the other, it was slightly tilted (3° to 5°) off the zenith (off zenith mode). Measurements were made in light rain as its Z_{DR} is zero at the zenith, and it is very close to zero in case of the slightly tilted principal plane. In either case, the differential phase equals the system differential phase. During the data collection in zenith mode, approximately 3 mm deep water layer accumulated on top of the radome. To avoid this water the antenna was tilted so that the principal plane was slightly off vertical thus allowing the water to drain off the radome. Two datasets revealed the effect of the thick uniform water layer on the radiation properties of the radar antenna and its effect on the calibration parameters. Here we illustrate measured differential reflectivity Z_{DR} and differential phase of the radar system (Fig. 2). In the first row (left) the radar operates in the zenith mode whereas at (right) it is off zenith. With antenna pointing at zenith (Fig. 2, left and steering angle 0°) the Z_{DR} should be zero, but it is -0.5 dB. This clearly is the system introduced bias that is increased with the pointing direction departing from the broadside to about 2 dB at about 45°. The increase of the differential reflectivity is expected due to the different nature of the H and V EM waves interaction with the radome. Namely, as the beam is steered in the H cardinal plane the H polarization has oblique incidence to the radome. At the same time, V polarization has the parallel incidence to the radome at all beam steering angles. This results in different "reductions" of the antenna gain through the radome at the twofor polarizations, thus the change in the differential gain. Another important feature is the Z_{DR} change in shape between the zenith and off zenith mode as well as the system Z_{DR} bias increase. The bias increase from about -0.5 to 1.3 dB can not be attributed to the antenna, and its origin remains to be determined.

Measurements of the differential phase Φ_{DP} are more consistent between two pointing directions than of the Z_{DR}. From the broadside value system differential phase is observed to be about 20°, whereas the electronic beam steering introduces the additional increas to 75° for zenith pointing or 55° for off zenith mode.

The next step in the calibration roadmap is the simulation of the full TPD antenna array. This is an intermediate step to the modeling of larger, operational PPARs. The TPD antenna is sufficiently "small" to be fully modeled and sufficiently large to serve as the test array in the development of the approximative techniques with sufficient accuracy for large/ full-scale operational PPAR array. This intermediate step is of utmost importance as the mathematical relationship between the various approximative techniques and the full solution can be established.

For replication of measured differential biases, we use two model setups. The first setup considers a single panel antenna with "dry" radome cover whereas the second one introduced additional water level on top of the radome ("wet" radome cover). The "wet" radome has a 3 mm thick layer of water representing the water layer on top of the radome in the zenith pointing mode. During weather surveillance, the radome would most likely be dry hence calibration for such condition is required. The situation with 3 mm uniform water film is highly unlikely for an operational radar, for which correction of the wet radome effects is applied differently].

To understand qualitatively the effects of the "wet" radome on the Z_{DR} and Φ_{DP} we chose to model beam steering on a single panel over 0 to 45° angle. The Fig. 3 shows the differential gain and differential phase of the antenna calculated at the beam peak for the case of "dry" and "wet" radome. Graphs include only steering for positive angles, as the symmetry of the calibration parameters is expected.

Simulated biases show the same trend as the biases estimated from the measured data. In both, we observe a significant difference between the "wet" and "dry" cases. Namely, the differential reflectivity bias for the radar pointing at zenith with the water layer on top of the radome has convex dependance on steering angle with Z_{DR} varying from 0.5 to 2.5 dB. The one-way differential gain in simulated data predicts a convex increase from about 0 to 6 dB; this is an overestimation most likely due to the water layer thickness. The differential gain for the dry radome has a variation of about 0.1 dB. The measurement, as aforementioned, at high elevation angle experiences concave behavior which is opposite to the simulation. This remains to be resolved.

The observed variation of the differential phase has a strong dependence on the pointing direction. Measured values show about 45° decrease of the differential phase for beam steering in zenith mode, and up to 30° when off zenith. The water layer in the simulation is overestimated. This is evident in the differential gain results (Fig. 3 (left)). This is most likely the cause of the differential phase's unexpected non-monotonic behavior. On the other hand, the results for the "dry" radome case are not just qualitatively correct but quantitatively as well. The simulation predicts approx 15° one-way (30° two way) differential phase from the antenna which agrees with the measured value if the system differential phase of about 20° is included.

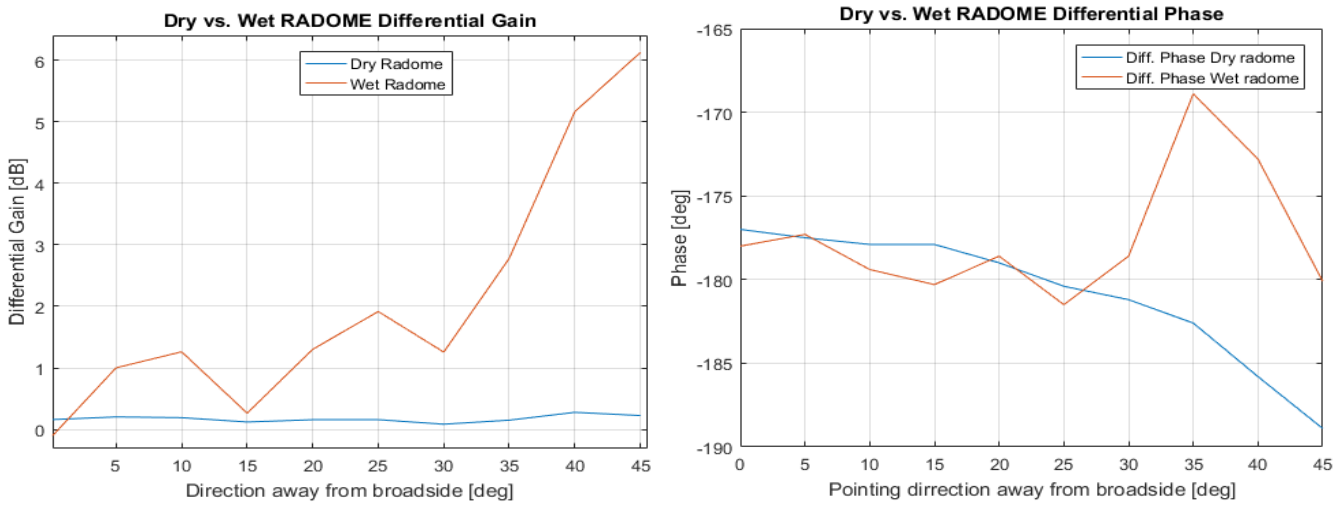

Fig. 3. The simulated differential gain (left) and differential phase(right) as polarimetric calibration parameters depicting variable bias due to the antenna and radome for "dry" and water covered(uniform 3mm layer of water) configuration. Simulated results present one-way (only transmision/reception) bias, while for the radar system this is cumulative effect of bias on transmission and reception (two-way).

VI. Conclusions

Using the CEM tools for simulation of antenna patterns is common practice, yet an application for polarimetric weather radar calibration of the antenna effects has not been made. Here we have demonstrated that the bias in differential reflectivity, in principle, can be obtained from the antenna model. We have also obtained the antenna's contribution to the offset of the system differential phase as a function of the beam pointing direction. Thus, both differential reflectivity and differential phase biases depend on the antenna pointing direction. It follows that for directions in the principal planes of the vertically oriented array (at S, C, and X bands) returns from any rain closest to the radar can be used to determine the total differential phase (i.e., contributions by the antenna and by the rest of the system). This is because the backscatter differential phase from rain is negligible at the frequencies of weather surveillance radars and thus would not influence the measurement. This is not so with differential reflectivity which depends heavily on the rain type. Therefore only light rain or drizzle with intrinsic Z_{DR} close to 0 dB is suitable for checking the total bias in Z_{DR}.

We have also identified issues in this ongoing work that need to be addressed before the final quantitative analysis can be carried out and inconsistencies in the radar observations which have to be corrected before high-quality data can be obtained. The development of the calibration procedure is expected to follow the path from a single panel model to a full-size antenna model. For large antennas, hybrid CEM methods need to be explored to find the ones that can achieve precise modeling of arrays with a few thousand elements.

VII. Acknowledgment

Authors would like to thank the MIT Lincoln Laboratory and Dr. Igor Ivic for the effort in radar design and data collection. Mr. Wasielewski was responsible for maintaining the TDP. Dr. R. Doviak comments helped to improve the manuscript. Funding was provided by NOAA/Office of Oceanic and Atmospheric Research under NOAA-University of Oklahoma Cooperative Agreement #NA11OAR4320072, U.S. Department of Commerce.

References

[1] P. L. Heinselman and S. M. Torres, "High-temporal-resolution capabilities of the national weather radar testbed phased-array radar," Journal of Applied Meteorology and Climatology, vol. 50, no. 3, pp. 579-593, 2011.

[2] G. Zhang, R. J. Doviak, D. S. Zrnic, J. Crain, D. Stainman, and Y. Al-Rashid, "Phased Array radar polarimetry for weather sensing: A theoretical formulation for bias corrections," IEEE Trans. on Geoscience and remote sensing, vol. 47, no. 11, pp. 3679-3689, 2009.

[3] D. S. Zrnic, R. J. Doviak, G. Zhang, Y. Zhang and C. Fulton, "Propagation and backscattering challenges for planar polarimetric phase array radars," in AMS Radar Conference Proceedings, Chicago, 2017.

[4] C. Fulton, J. Salazar, D. Zrnic, D. Mirkovic, I. Ivic, and R. Doviak, "Polarimetric Phased Array Calibration for Large Scale Multi-Mission Radar Applications," in Proc. IEEE Radar, Oklahoma City, 2018.

[5] L. Lei, G. Zhang, R. J. Doviak, and S. Karimkashi, "Comparison of theoretical biases in estimating polarimetric properties of precipitation with weather radar using parabolic reflector, or planar and cylindrical arrays," Trans. on Geoscience and Remote Sensing, vol. 53, no. 8, pp. 4313-4327, 2015.

[6] V. Bringi and V. Chandrasekar, Polarimetric Doppler Weather Radar: Principles and Applications. Cambridge University Press, 2001.

[7] M. Sachidananda and D. S. Zrnic, "Rain rate estimates from differential polarization measurements," J. Atmos. Oceanic Tech., vol. 4, pp. 588-598, 1977.

[8] N. Balakrishnan and D. S. Zrnic, "Use of polarization to characterize precipitation and discriminate large hail," J. Atmos. Sci., pp. 1525-1540, 1990.

[9] A. Mancini, J. Salazar, R. Lebron, and B. Leng Cheong, "A novel technique to characterize the effect of rain over a radome for radar applications," in IEEE Radar Conference 2017, Seattle, 2017.